Langmuir

Article

pubs.acs.org/Langmuir

Circular Dichroism Analysis of Cyclic β-Helical Peptides Adsorbed on Planar Fused Quartz

Kenan P. Fears,*[,†] Dmitri Y. Petrovykh,[†,‡,§] Sara J. Photiadis,[†] and Thomas D. Clark*[,†]

[†]Division of Chemistry, Naval Research Laboratory, Washington, District of Columbia 20375, United States

[‡]Department of Physics, University of Maryland, College Park, Maryland 20742, United States

ABSTRACT: Conformational changes of three cyclic β-helical peptides upon adsorption onto planar fused-quartz substrates were detected and analyzed by far-ultraviolet (UV) circular dichroism (CD) spectroscopy. In trifluoroethanol (TFE), hydrophobic peptides, **Leu *β*** and **Val *β***, form left- and right-handed helices, respectively, and water-soluble peptide **WS *β*** forms a left-handed helix. Upon adsorption, CD spectra showed a mixture of folded and unfolded conformations for **Leu *β*** and **Val *β*** and predominantly unfolded conformations for **WS *β***. X-ray photoelectron spectroscopy (XPS) provided insight about the molecular mechanisms governing the conformational changes, revealing that ca. 40% of backbone amides in **Leu *β*** and **Val *β*** were interacting with the hydrophilic substrate, while only ca. 15% of the amines/amides in **WS *β*** showed similar interactions. In their folded β-helical conformations, **Leu *β*** and **Val *β*** present only hydrophobic groups to their surroundings; hydrophilic surface groups can only interact with backbone amides if the peptides change their conformation. Conversely, as a β helix, **WS *β*** presents hydrophilic side chains to its surroundings that could, in principle, interact with hydrophilic surface groups, with the peptide retaining its folded structure. Instead, the observed unfolded surface conformation for **WS *β*** and the relatively small percentage of surface-bound amides (15 versus 40% for **Leu *β*** and **Val *β***) suggest that hydrophilic surface groups induce unfolding. Upon this surface-induced unfolding, **WS *β*** interacts with the surface preferentially via hydrophilic side chains rather than backbone amides. In contrast, the unfolded β-hairpin-like form of **WS *β*** does not irreversibly adsorb on fused quartz from water, highlighting that solvation effects can be more important than initial conformation in governing peptide adsorption. Both label-free methods demonstrated in this work are, in general, applicable to structural analysis of a broad range of biomolecules adsorbed on transparent planar substrates, the surface properties of which could be customized.

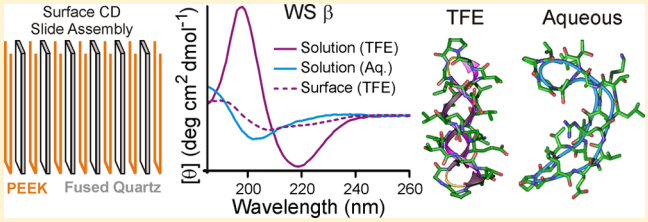

INTRODUCTION

Understanding the interactions between proteins and surfaces is a long-standing goal of biointerfacial science, motivated by the critical importance of structure−function relationships in determining biomolecular recognition and activity.[1−4] The observation that proteins typically undergo changes in secondary structure upon adsorption to surfaces suggests that examining such changes will shed light on the molecular mechanisms of adsorption. However, the complexity of proteins and the challenges inherent to studying molecules at interfaces complicate the detailed study of protein conformational changes on surfaces. One approach to overcoming these complications is to use model peptides that are smaller and less complex than typical proteins but that, nonetheless, exhibit well-defined conformations in solution.

We selected cyclic β-helical peptides as model peptides for this study because of their well-defined conformations and their tendency to maintain a monomeric, unaggregated structure in solution.[5−9] This last property is crucial because we sought to examine the adsorption of individual peptides from solution rather than the adsorption and/or precipitation of peptide aggregates. In addition, cyclic β helices have several features in common with other peptide secondary structures. Based on α-amino-acid peptide backbones, cyclic β helices are stabilized by hydrogen bonds and can, in principle, be further stabilized by additional non-covalent interactions, including salt bridges. Together, these properties of cyclic β-helical peptides offered a well-defined starting point for discerning surface-induced changes in the secondary structure of the peptides after adsorption. We examined two hydrophobic peptides designed to form β helices of opposite handedness,[5,7,8] **Leu *β*** (left-handed) and **Val *β*** (right-handed), as well as one hydrophilic peptide (**WS *β***) that forms a left-handed helix.[6] While **Leu *β*** and **Val *β*** possess only hydrophobic residues, **WS *β*** contains eight polar residues—including two side-chain-to-side-chain ion pairs—distributed uniformly along the outside of the helix (Figure 1). By comparing hydrophobic and hydrophilic model peptides, we were able to assess the role of hydrophilicity in peptide adsorption. In addition, our prior work had shown that peptide **WS *β*** adopts β-helical and β-hairpin-like conformations in trifluoroethanol (TFE) and water, respectively, a property that allowed us to scrutinize the adsorption behavior of the

Received: April 25, 2013
Revised: June 16, 2013
Published: July 11, 2013

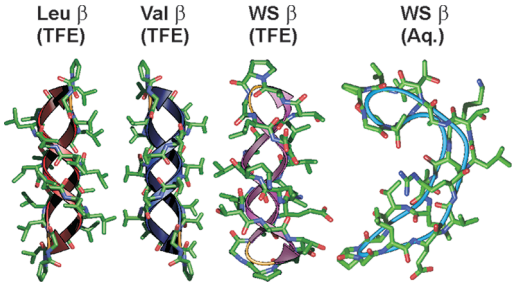

Figure 1. Spectroscopically derived structures of the model cyclic peptides, each consisting of 22 amino acids. The two hydrophobic peptides, *cyclo*{[(L-Leu−D-Leu)$_4$−(L-Leu−D-Pro−Gly)]$_2$−} (**Leu *β***, left-handed) and *cyclo*{[(D-Val−L-Val)$_4$−(D-Val−L-Pro−Gly)]$_2$−} (**Val *β***, right-handed),[5] adopt *β*-helical conformations in TFE. The water-soluble peptide, *cyclo*[(D-Ala−L-Glu−D-Leu−L-Lys−D-Val−L-Thr−D-Leu−L-Thr−D-Ala−L-Pro−Gly−D-Leu−L-Glu−D-Val−L-Arg−D-Leu−L-Thr−D-Ala−L-Thr−D-Val−L-Pro−Gly)−] (**WS *β***), is also *β*-helical in TFE but becomes *β*-hairpin-like in an aqueous buffer.[6]

peptide as a function of solvent and initial solution conformation.

We chose fused quartz as a model substrate because of its transparency to ultraviolet (UV) light, which, in turn, allowed us to use far-UV circular dichroism (CD) spectroscopy [also known as electronic circular dichroism (ECD)] as our primary method to assess peptide conformational changes. CD is well-known as an effective technique for analyzing the secondary structure of proteins and peptides *in solution*,[10,11] where the solute concentration and optical path length can be optimized for efficient signal collection. Similar approaches have been used to extend CD to measurements of peptides adsorbed on micro- and nanoparticle surfaces, where the particles provide a large surface area and ease of solution manipulation.[12−18] CD analysis of protein and peptide monolayers on technologically important planar substrates, however, is limited by the low effective concentration or small number of molecules in the optical path. For proteins, these limitations had been overcome in the past by stacking substrates to increase the effective protein concentration in the optical path.[19−26] Here, we present an extension of this simple yet versatile method to assess the secondary structure of small peptides irreversibly adsorbed as sub-monolayers on planar fused-quartz surfaces.

We used the peptide absorbance band at 195 nm to quantify the effective peptide concentration in the optical path;[25−27] in addition, we used X-ray photoelectron spectroscopy (XPS) as a complementary technique to verify irreversible adsorption of the peptides and quantify their relative surface densities. Examining the N 1s XPS spectra also allowed us to detect amide nitrogens in peptides that are strongly interacting with inorganic substrates,[28−30] furnishing mechanistic information concerning the adsorption of small model peptides.

EXPERIMENTAL SECTION

Model Peptides. Cyclic *β*-helical peptides **Leu *β*** and **WS *β*** were available from prior studies.[6,7] We synthesized **Val *β*** using an improved version of our earlier method by beginning with a glycine-loaded resin, H-Gly-sulfamylbutyryl NovaSyn TG resin, rather than the D-Val-sulfamylylbutyryl AM resin used previously, to avoid epimerization during the cleavage-by-cyclization step.[7]

Peptide Adsorption. We obtained ground and polished fused quartz slides (30.0 × 9.5 × 0.63 mm) from Chemglass (Vineland, NJ). The slides were sequentially sonicated for 5 min in each of the following solutions: 0.005% (v/v) Triton X-100, "Piranha" wash (7:3 H_2SO_4/H_2O_2), and RCA standard clean 1 (1:1:5 $NH_4OH/H_2O_2/H_2O$) (note that Piranha solution must be handled with care; it is extremely oxidizing, reacts violently with organics, and should only be stored in loosely tightened containers to avoid pressure buildup). The slides were rinsed thoroughly with 18 MΩ H_2O after each cleaning solution and, at the completion of the cleaning process, dried under a stream of nitrogen gas. We cleaned the slides immediately prior to peptide adsorption experiments to limit the surface adsorption of atmospheric carbonaceous contaminants. Because all three peptides are soluble in TFE, TFE was selected as the solvent for all adsorption experiments. Cleaned fused quartz slides were placed in a polytetrafluoroethylene (PTFE) incubation chamber filled with TFE, and then the appropriate amount of peptide stock solution was added to yield a 0.2 mM incubation concentration. We followed this order of addition to prevent transferring the slides through an air−liquid interface, where peptides could accumulate.[31] Likewise, at the end of the incubation period, we filled the chamber to overflowing with copious amount of TFE, in effect, infinitely diluting the incubation solutions before removing and rinsing the slides to remove loosely bound peptides. The PTFE incubation chamber was designed to promote the uniform adsorption of peptides on both sides of the fused quartz slides and to minimize solvent evaporation during incubation. In preliminary adsorption experiments, we did not observe a significant difference in the surface density of irreversibly adsorbed peptides between 18 and 24 h; thus, we selected incubation periods of 24 h to achieve quasi-equilibrium surface densities prior to the CD analysis.

CD Spectroscopy. We used a Jasco J-815 spectrometer to simultaneously collect UV absorbance and ECD spectra over the wavelength range of 185−260 nm. The temperature was held constant at 20 °C by a Peltier controller during spectral scans to minimize solvent evaporation and temperature fluctuations. Control CD spectra in solution were collected for **Leu *β*** and **Val *β*** in TFE and trifluoroacetic acid (TFA) and for **WS *β*** in TFE and 10 mM sodium phosphate at a scan rate of 50 nm/min, with three accumulations being averaged to establish the characteristic spectral features for the peptides in their folded (TFE) and unfolded (TFA and aqueous) states. We used a 1.0 mm path-length quartz cuvette for solution controls in TFE and in 10 mM sodium phosphate buffer, adjusted to pH 7.0 by mixing the appropriate amount of 10 mM NaH_2PO_4 and Na_2HPO_4 solutions; for solution controls in TFA, we used a 10 *μ*m path-length cuvette.

We selected the dimensions of the fused quartz slides (30.0 × 9.5 × 0.63 mm) to fit inside standard open-top cuvettes while leaving a solvent reservoir above the slides to prevent the formation of air pockets between the slides during CD analysis because of solvent evaporation. All adsorption spectra were collected in TFE using assemblies of 13 fused quartz slides and 14 spacers [75 *μ*m thick polyetheretherketone (PEEK)] in a 1.0 cm path-length cuvette (Figure 2). The PEEK spacers were cut out of a large PEEK sheet (K-mac Plastics) and cleaned in a solution of dish detergent followed by rinses with 18 MΩ H_2O and acetone. CD scans were acquired at 10 nm/min with three accumulations being averaged for each independent adsorption experiment. Surface spectra reported herein are the average of at least three independent adsorption experiments.

We applied baseline corrections to all CD and UV absorbance spectra by subtracting background spectra collected with the cuvette and slide assembly, as shown in Figure 2, but using blank solvent containing no peptide. Baseline-corrected CD spectra were converted from raw ellipticity (θ, mdeg) to mean molar ellipticity per residue ($[\theta]$, deg cm^2 dmol^{-1}) to correct for the concentration using the following equations for solution and adsorption studies, respectively:

$$[\theta] = \frac{\theta \times \mathrm{MW}}{10000 \times C_{\mathrm{soln}} \times L \times N} \quad \text{or} \quad \frac{\theta \times \mathrm{MW}}{10000 \times C_{\mathrm{ads}} \times N}$$

where MW is the molecular weight of the peptide (g mol^{-1}), C_{soln} is the peptide concentration in solution (g mL^{-1}), L is the optical path length through solvent (cm), N is the number of residues (22), and C_{ads} is the surface concentration of peptide (g cm^{-2}).

dx.doi.org/10.1021/la401544c | *Langmuir* 2013, 29, 10095−10101

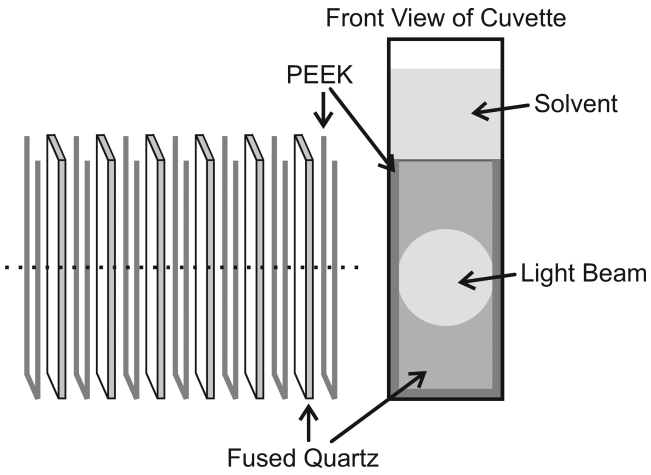

Figure 2. Diagram of the slide/spacer assembly used for CD analysis. Stacks of 13 slides (30.0 × 9.5 × 0.63 mm) separated by 75 μm thick U-shaped PEEK spacers were assembled in standard 1.0 cm quartz cuvettes.

We calculated the peptide concentrations, solution and surface-adsorbed, using the peptide absorbance peak at 195 nm (A_{195}), in accordance with previous literature.[25−27] We constructed calibration curves for each of the peptides examined in this study using serial dilutions of peptide stock solutions, whose concentrations were determined by the nominal weight of purified peptide added to the solvent. The extinction coefficients (ε_{195}, mL g^{-1} cm^{-1} or cm^2 g^{-1}), as determined by the calibration curves, were used to calculate peptide concentrations based on Beer's law relationship.

$$A_{195} = \varepsilon_{195} \times C_{soln} \times L \quad \text{or} \quad \varepsilon_{195} \times C_{ads}$$

XPS. Elemental and chemical state surface analyses were performed using a commercial XPS spectrometer equipped with a monochromatic Al Kα source microfocused to a spot size of ca. 400 × 600 μm^2 on the sample. The energy of the Al Kα X-ray source was regularly calibrated and maintained at 1486.6 ± 0.2 eV. The binding energy (BE) scale of the spectrometer was regularly calibrated using an automated procedure that produced the Au 4f$_{7/2}$, Cu 2p$_{3/2}$, and Ag 3d$_{5/2}$ peaks within <0.05 eV from the standard reference BE values.[32] Charge neutralization of the insulating surfaces was provided by beams of low-energy (≤10 eV) electrons and Ar$^+$ ions. The aliphatic C 1s peak was observed at BE = 284.7 ± 0.2 eV for peptide samples. We analyzed the fused quartz slides after 24 h incubations in either blank solvent or 0.2 mM peptide solutions. We analyzed a minimum of three slides for each adsorption condition and at least three separate spots on each slide. XPS data were acquired at room temperature in an ultrahigh vacuum analysis chamber with the base pressure of <5 × 10^{-9} mbar. Scans were carried out at 200 and 20 eV pass energies for elemental survey and high-resolution scans, respectively. High-resolution scans (0.15 eV step size at ca. 0.5 eV resolution) were acquired for the Si 2p, C 1s, N 1s, O 1s, and F 1s regions to determine the stoichiometry and surface coverage of the adsorbed peptides. Peaks in the high-resolution spectra were fit using a convolution of Lorentzian and Gaussian line shapes in Unifit for Windows (version 2011). Elemental N/Si ratios were normalized by the average number of nitrogen atoms per residue to determine the relative surface density of peptide residues irreversibly adsorbed to the substrates.

RESULTS AND DISCUSSION

In Figure 1, we show the NMR-derived structures of **Val** $\boldsymbol{\beta}$[5] and **WS** $\boldsymbol{\beta}$.[6] These structures were determined from NMR data obtained in chloroform and methanol (MeOH) solutions, respectively; nevertheless, the CD spectra of **Val** $\boldsymbol{\beta}$ in chloroform and TFE are nearly identical, as are those of **WS** $\boldsymbol{\beta}$ in MeOH and TFE. These observations gave us confidence that the structures shown in Figure 1 are similar to the structures of the peptides in TFE. We inferred the structure of **Leu** $\boldsymbol{\beta}$ from the similarity of its 1D and 2D NMR spectra to those of **Val** $\boldsymbol{\beta}$[5] and from the observation that the CD[5] and vibrational circular dichroism (VCD)[8] spectra of **Leu** $\boldsymbol{\beta}$ are nearly equal in magnitude but opposite in sign to those of **Val** $\boldsymbol{\beta}$, as expected for β helices having similar conformations but opposite handedness.

The results of the adsorption experiments and solution controls for the hydrophobic helices are shown in Figure 3. The CD spectra of both **Leu** $\boldsymbol{\beta}$ and **Val** $\boldsymbol{\beta}$ exhibit bands characteristic of β helices, with extrema at ca. 198 and 218 nm.[5,33,34] The solution spectra are similar in magnitude but opposite in sign, indicating that the peptides form nearly identical left-handed (**Leu** $\boldsymbol{\beta}$) and right-handed (**Val** $\boldsymbol{\beta}$) helices.[5,35] Likewise, we observed that the similarity of their solution properties translated to the adsorption behavior of these peptides, yielding surface CD spectra that resembled each other, aside from the reversal in sign. We note that the observation of adsorbed peptide even after extensive rinsing with TFE (as described in the Experimental Section) indicates that the peptides are adsorbed irreversibly under these experimental conditions. While the characteristic helical bands were present in the spectra of the adsorbed peptides, on the basis of the reduction of the bands at 218 nm, both peptides underwent a substantial loss of helicity upon adsorption. Because CD is a measure of the average structure, we do not know the number or distribution of unfolded states present on the surface. The shift in extrema below 200 nm in the surface spectra is most likely due to differences in the distribution of unfolded states in the adsorbed peptide layers. We note that CD has been shown to be sensitive to the orientation of α-helical peptides; in particular, a decrease in signal intensity and shifts in spectral features can be observed for helices aligned perpendicular to the surface.[36,37] In our study, however, all surface-adsorbed spectra were collected with the substrates fixed normal to the incident beam and the surface coverages of **Leu** $\boldsymbol{\beta}$ and **Val** $\boldsymbol{\beta}$, as determined by UV absorbance, were consistent with the theoretical coverage of a monolayer of the peptides adsorbed in a side-on orientation, 90 ± 18% saturated. Furthermore, the positions of the bands are consistent between the solution and surface spectra in TFE. These observations gave us confidence that the reductions in signal intensities between the solution and surface spectra were due to conformational changes rather than the peptides preferentially absorbing with their helical axes normal to the surface.

Because we had not previously obtained CD spectra of the hydrophobic peptides in an unfolded state, we sought to induce the unfolding of **Leu** $\boldsymbol{\beta}$ and **Val** $\boldsymbol{\beta}$ to test whether or not their surface CD spectra (Figure 3) are consistent with conformation intermediates between β-helical and unfolded (random coil). We induced unfolding by dissolving the hydrophobic peptides in TFA; the resulting CD spectra were characteristic of a random coil (Figure 3).[10] For both peptides, the three CD spectra—random-coil in TFA, β-helical in TFE, and surface-adsorbed—exhibited an isosbestic point (also known as an isodichroic point) at ca. 208 nm, showing that the average conformation of the surface-adsorbed state is consistent with a linear combination of β-helical and random-coil structures.[38] We fit each surface-adsorbed spectrum to a linear combination of the spectra in TFE and TFA by minimizing the sum of the squared errors (SSE) to estimate the degree of unfolding upon surface adsorption, similar to the concept established by

dx.doi.org/10.1021/la401544c | Langmuir 2013, 29, 10095−10101

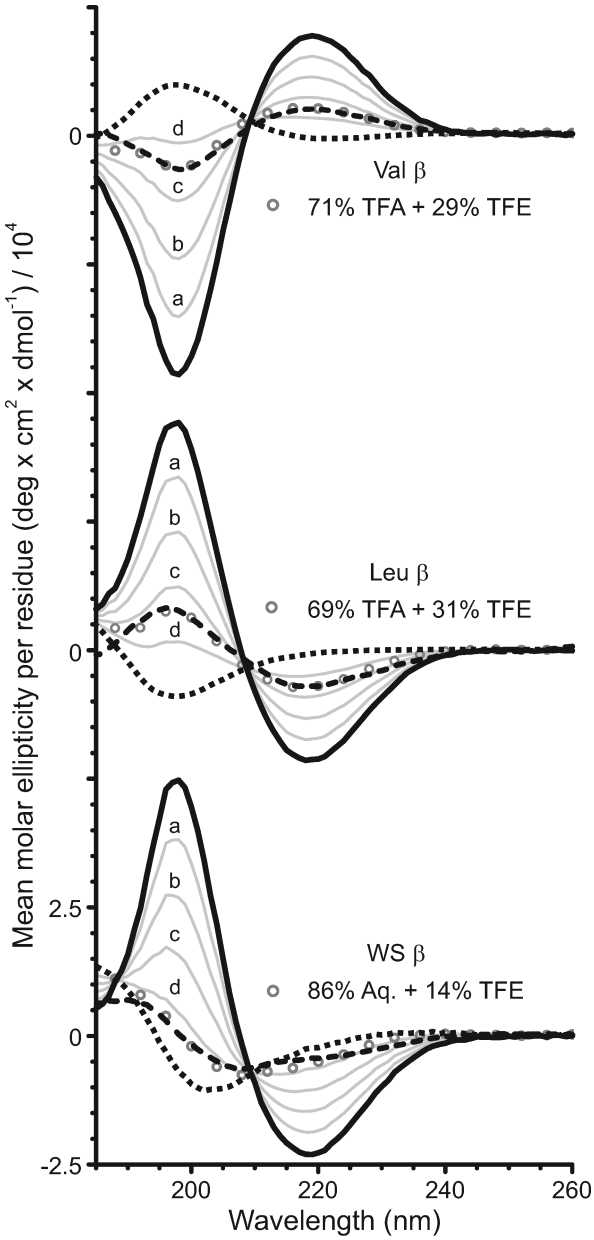

Figure 3. Solution and surface-adsorbed CD spectra of β-helix-forming peptides. Solution spectra are shown for 2 mM peptide solutions of **Val** $\boldsymbol{\beta}$ and **Leu** $\boldsymbol{\beta}$ in TFE (solid lines) and TFA (dotted lines) and **WS** $\boldsymbol{\beta}$ in TFE (solid line) and aqueous phosphate buffer (dotted line). To obtain surface-adsorbed spectra (dashed lines), fused-quartz slides were incubated for 24 h in 0.2 mM peptide solutions (TFE). The gray lines represent linear combinations of the reference solution spectra with (a) 80%, (b) 60%, (c) 40%, and (d) 20% contributions from the TFE spectra, and the gray circles represent the best-fit, linear combination.

Greenfield and Fasman for evaluating protein conformations.[10] On the basis of these fits, we found that surface-adsorbed **Leu** $\boldsymbol{\beta}$ and **Val** $\boldsymbol{\beta}$ molecules retained ca. 30% of their helicity post-adsorption.

We observed a stark difference in the adsorption behavior of the hydrophilic **WS** $\boldsymbol{\beta}$ in comparison to that of the hydrophobic helices. None of the characteristic β-helical peaks were present in the spectra of **WS** $\boldsymbol{\beta}$ post-adsorption; rather, its spectra resembled the peptide in an aqueous buffer (Figure 3), where previous NMR analysis indicated β-hairpin-like conformations for **WS** $\boldsymbol{\beta}$.[6] On the basis of the best-fit linear combination of the corresponding reference solution spectra, we estimated that **WS** $\boldsymbol{\beta}$ retained ca. 14% of its helicity post-adsorption, as compared to ca. 30% for **Leu** $\boldsymbol{\beta}$ and **Val** $\boldsymbol{\beta}$.

Leu $\boldsymbol{\beta}$ and **Val** $\boldsymbol{\beta}$ are uniformly hydrophobic and form β helices in hydrophobic solvents, including TFE (Figure 3). In contrast, **WS** $\boldsymbol{\beta}$ contains eight polar residues and forms β helices not only in TFE but also in the more hydrophilic solvent MeOH. The β-helical structure of **WS** $\boldsymbol{\beta}$ in MeOH contains, by design, two side-chain-to-side-chain ion pairs. In aqueous buffer, however, these two ion pairs are insufficient to stabilize a β-helical conformation, and the peptide instead adopts a β-hairpin-like conformation, in which hydrophilic side chains and backbone amide groups are solvated by water molecules. Fused-quartz surfaces may serve a similar role to that of water, promoting the unfolding of **WS** $\boldsymbol{\beta}$ into a β-hairpin-like conformation, in which the hydrophilic side chains can enjoy maximum "solvation" by surface silanol groups. Electrostatic interactions between the basic residues Arg and Lys in **WS** $\boldsymbol{\beta}$ and the acidic surface silanol groups may also disrupt ion pairs and destabilize the helical structure. As detailed in our earlier work,[6] we were unable to assess the energetics of folding/unfolding for **WS** $\boldsymbol{\beta}$ because the peptide did not undergo thermal denaturation at experimentally accessible temperatures. Consistent with these experimental findings, Meier and van Gunsteren reported that, from molecular dynamics simulations, the thermal denaturation temperature of **Val** $\boldsymbol{\beta}$ is between 700 and 780 K.[9]

Conversely, the hydrophilic silanol groups on quartz surfaces may be responsible for the higher degree of β-helical structure in hydrophobic peptides **Leu** $\boldsymbol{\beta}$ and **Val** $\boldsymbol{\beta}$ (ca. 30%) with respect to **WS** $\boldsymbol{\beta}$ (ca. 14%). We hypothesize that the silanol-covered quartz surfaces induce a quasi-"solvophobic" stabilization of the compact, β-helical forms **Leu** $\boldsymbol{\beta}$ and **Val** $\boldsymbol{\beta}$, in which the exposed surface area of hydrophobic side chains is minimized.

Despite unfolding upon surface adsorption from TFE, **WS** $\boldsymbol{\beta}$ did not irreversibly adsorb to fused quartz from aqueous buffer (Figure 4). In one sense, this result may appear counterintuitive because the unfolded, β-hairpin-like conformation of **WS** $\boldsymbol{\beta}$ in water may be considered "preorganized" for adopting the unfolded state observed for the peptide adsorbed from TFE. We note, however, that water is much more polar than TFE; for example, the ratio of dielectric constants of water to TFE is ca. 3:1.[39] This difference in polarity likely reduces the relative strength of polar contacts between the peptide and the quartz silanol groups and prevents adsorption from water. These observations underscore the important role that solvation effects can play in peptide adsorption from solution.

Following CD analysis, we selected a number of slides for XPS analysis, to provide further insight into adsorption of these peptides (Table 1). We observed the characteristic peptide XPS peaks in the N 1s and C 1s regions (Figure 4) that were collected from randomly selected slides after CD analysis.[29,40,41] Interestingly, we detected the presence of TFE, as revealed by the C5 component, on substrates with surface-adsorbed peptides but not on the TFE control, indicating that TFE molecules are trapped by or adsorbed to peptide molecules; interference from the TFE bands in the amide region rendered these surfaces unsuitable for analysis by attenuated total reflectance infrared (ATR-IR) spectroscopy.

Because there were no adventitious nitrogen species detected on the blank TFE control, we calculated relative surface

dx.doi.org/10.1021/la401544c | Langmuir 2013, 29, 10095−10101

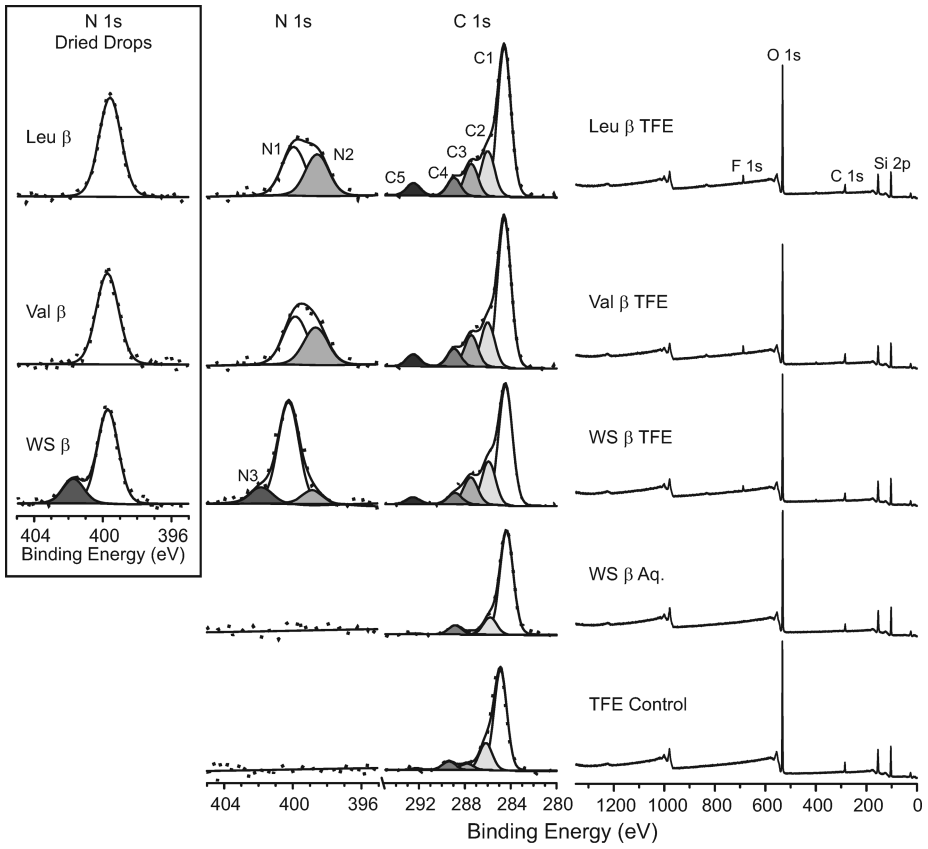

Figure 4. XPS data for peptides adsorbed on fused-quartz surfaces. (Center) High-resolution spectra of the N 1s (4× intensity shown for clarity) and C 1s regions are shown with peak components shaded: N1 (amide group), N2 (surface-bound amide/amine group), and N3 (protonated amine group) and C1 (C−C), C2 (C−O or C−N), C3 (C═O), C4 (O−C═O or N−C═O), and C5 (CF_3). (Right) XPS survey spectra of fused-quartz slides after incubating for 24 h in pure TFE (TFE control, bottom) or in 0.2 mM solutions of the indicated peptide in the indicated solvent. (Inset, left) Normalized high-resolution N 1s spectra of thick peptide films formed on fused-quartz slides by drying drops of 2 mM peptide stock solutions in TFE.

Table 1. Elemental Compositions (Atomic Percentage), as Measured by XPS, of Fused-Quartz Slides after Incubating in 0.2 mM Peptide Solutions for 24 h [$n \geq 9$; Mean ± 95% Confidence Interval (CI)]

	peak (eV)	**Leu *β*** TFE	**Val *β*** TFE	**WS *β*** TFE	**WS *β*** aqueous	TFE control
C 1s		12.5 ± 2.6	15.1 ± 1.3	10.9 ± 1.5	8.0 ± 0.7	8.5 ± 0.9
C1	284.6	7.1 ± 1.6	8.9 ± 0.9	6.5 ± 0.6	6.4 ± 0.4	6.7 ± 0.8
C2	286.0	2.2 ± 0.5	2.8 ± 0.2	2.0 ± 0.5	1.1 ± 0.2	1.0 ± 0.1
C3	287.5	1.6 ± 0.2	1.8 ± 0.1	1.3 ± 0.3		0.2 ± 0.1
C4	289.0	0.8 ± 0.2	1.0 ± 0.1	0.7 ± 0.1	0.5 ± 0.1	0.6 ± 0.1
C5	292.5	0.7 ± 0.1	0.6 ± 0.1	0.4 ± 0.1		
N 1s		1.0 ± 0.1	1.03 ± 0.04	1.2 ± 0.3		
N1	399.8	0.50 ± 0.03	0.6 ± 0.1	0.8 ± 0.2		
N2	398.5	0.41 ± 0.05	0.40 ± 0.04	0.2 ± 0.1		
N3	401.3			0.2 ± 0.1		
O 1s	532.2	54.6 ± 2.4	52.1 ± 0.8	54.4 ± 1.1	58.1 ± 1.0	58.4 ± 1.1
Si 2p	102.9	30.0 ± 1.0	29.8 ± 0.5	31.2 ± 0.8	33.9 ± 0.8	33.1 ± 0.9
F 1s	688.4	2.0 ± 0.1	2.0 ± 0.2	1.4 ± 0.1		

densities by normalizing the atomic N/Si ratios by the number of nitrogen atoms per residue, 1.00 for **Leu *β*** and **Val *β*** and 1.18 for **WS *β***, which has two residues with nitrogen-containing side chains, Arg and Lys, yielding values of 0.033 ± 0.006, 0.034 ± 0.003, and 0.032 ± 0.006 for **Leu *β***, **Val *β***, and **WS *β***, respectively. Metwalli et al. report a N/Si ratio of 0.046 for (3-aminopropyl)triethoxysilane (APS) monolayers on fused quartz,[42] which have a reported packing density of 6.4 molecules (or nitrogen atoms) per nm^2.[43] From molecular models of their *β*-helical conformations, we calculated that **Leu *β***, **Val *β***, and **WS *β*** molecules would have a footprint of approximately 3.6 nm^2 if adsorbed side-on or 1.1 nm^2 if adsorbed end-on; thus, 6.1 or 20.0 nitrogen atoms per nm^2 for the hydrophobic helices adsorbed side-on or end-on, respectively, and 7.2 or 23.6 nitrogen atoms per nm^2 for **WS *β*** adsorbed side-on or end-on, respectively. On the basis of the reported APS surface density and theoretical peptide densities, fully saturated monolayers of peptides adsorbed side-on versus

dx.doi.org/10.1021/la401544c | *Langmuir* 2013, 29, 10095−10101

end-on would have normalized N/Si ratios of 0.044 versus 0.143, respectively. Our previous assertion that the peptides adsorbed side-on is reinforced by the low normalized N/Si ratios measured by XPS with respect to the theoretical ratio for a monolayer of peptides adsorbed end-on. Using the theoretical ratio for side-on adsorption, we estimated that the surface was 75, 77, and 73% saturated for **Leu** β, **Val** β, and **WS** β, respectively, highlighting that differences in the surface-CD spectra (Figure 5) are unlikely to be attributable to variations in surface densities among the peptides.

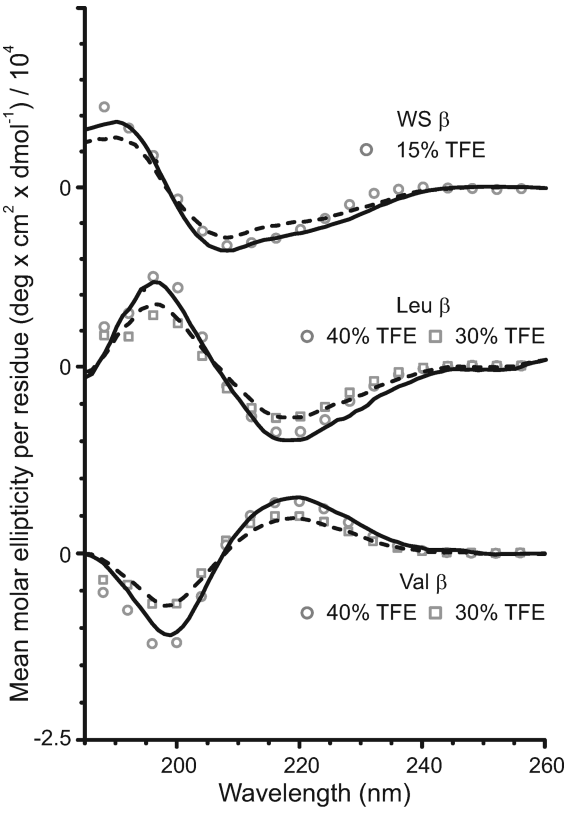

Figure 5. Normalization and fitting of surface CD spectra. Surface-adsorbed CD spectra were collected in TFE from fused-quartz slides that were incubated for 24 h in 0.2 mM peptide solutions. Spectra were converted from raw ellipticity according the surface concentrations determined by UV absorbance (dashed lines) or XPS (solid lines). The gray symbols represent linear combinations of the reference solution spectra in TFE and TFA for **Leu** β and **Val** β and TFE and an aqueous phosphate buffer for **WS** β.

While we detected no statistical difference in surface coverage between the different adsorbed peptide layers, there was a large disparity in the N 1s component centered at BE ≈ 398.5 eV; we note that this BE corresponds to nitrogen atoms interacting strongly with inorganic substrates via contacts that involve significant charge transfer.[28,30,44] To ensure that the observation of this component is due solely to peptide−surface interactions, as a control, we deposited thick peptide films on fused-quartz slides by drying multiple drops of 2 mM peptide (dissolved in TFE). Figure 4 shows that only the N1 component, corresponding to backbone amide groups, was observed for the hydrophobic peptides, and only the N3 component, corresponding to protonated side chains of Arg or Lys, was observed for **WS** β in addition to the N1 component. The relative areas of the N 1s components in Figure 4 suggest that ca. 40% of backbone amide nitrogens in the hydrophobic peptides, in contrast to ca. 15% in the hydrophilic **WS** β, interact with the fused-quartz surface. This difference likely arises from the differences in residue composition among the peptides influencing how they interact with the surface. As noted above, **Leu** β and **Val** β comprise only hydrophobic residues, while **WS** β contains eight polar residues, including one Lys and one Arg, uniformly distributed along the outside of the helix. Thus, **Leu** β and **Val** β can only make polar contacts with the surface via their peptide backbones, while **WS** β can make polar contacts both via its peptide backbone and its polar side chains. For **WS** β, interactions of the polar side chains with the quartz surface may be more energetically favorable than corresponding interactions involving the peptide backbone. According to this line of reasoning, **WS** β undergoes a conformational change from a compact helix to a more extended, unfolded structure to maximize interactions between the uniformly distributed polar side chains and the polar quartz surface. Because the side chains of peptides in a helical conformation point outward (Figure 1), even hydrophobic peptides **Leu** β and **Val** β must undergo conformational changes to present their polar peptide backbones to the polar surface to minimize the interaction energy. These conformational changes likely prevent the peptides from refolding into helices once adsorbed.

The apparent strong interactions (indicated by BE-shifted N2 components in Figure 4) between the peptides and surface raise the question of whether or not these interactions alter the molar extinction coefficient, an effect that could explain the higher surface coverages and the variance of the values determined by UV absorbance versus those calculated by XPS. We assessed the potential importance of this effect by comparing the mean molar ellipticity per residue calculated using the coverages derived by the two methods. We observed a small difference between the linear combination fittings for **WS** β, 14% when normalized by UV absorbance and 15% when normalized by XPS coverage. In contrast, we calculated a 7% increase in the estimated helicity of surface-adsorbed **Leu** β and **Val** β when we used the coverages from XPS rather than UV absorbance, 38 versus 31% and 36 versus 29%, respectively. Clearly, the apparent percent helicity of the surface-adsorbed peptides depends to some extent upon the method used to determine surface coverage. In either case, however, our conclusions remain the same: the hydrophobic peptides **Leu** β and **Val** β retain significantly greater helicity upon surface adsorption than does the hydrophilic peptide **WS** β.

CONCLUSION

The methods described here proved effective in label-free analysis of peptide secondary structure after adsorption on fused-quartz substrates. These methods represent a versatile approach to interrogating biomolecular structure of a wide variety of biomolecules on planar surfaces, because the substrate thickness, spacer thickness, and cuvette path length can be readily changed to meet experimental needs. In addition to conformational information obtained from CD spectroscopy, we gained insight about underlying adsorption mechanisms through complementary XPS analysis. As expected, the peptides appear to interact with the hydrophilic surface via hydrophilic peptide chemistries, but the adsorption behavior is strongly affected by solvation effects, as shown by the inability of **WS** β to irreversibly adsorb from its unfolded, β-hairpin-like conformation in aqueous buffer.

dx.doi.org/10.1021/la401544c | *Langmuir* 2013, 29, 10095−10101

Irreversible adsorption of **Leu β** and **Val β** appears to involve polar contacts between backbone amides and the surface. In contrast, **WS β** appears to interact with the surface mainly via its polar side chains. These inferences are derived from XPS experiments, which identified only 15% of the nitrogen atoms in **WS β**, some of which could be from Lys and Arg side chains, as strongly interacting with the surface versus 40% of the amide nitrogens in the hydrophobic peptides. **Leu β** and **Val β** retained more of their helicity than did **WS β**; we hypothesize that the differences in interaction affinity of the hydrophobic and hydrophilic side chains, respectively, with the hydrophilic silanol-covered surface partially stabilize the hydrophobic β helices through "solvophobic" interactions while destabilizing the hydrophilic β helix by "solvating" hydrophilic side chains.

AUTHOR INFORMATION

Corresponding Author

*E-mail: kenan.fears@nrl.navy.mil (K.P.F.); thomas.clark@nrl.navy.mil (T.D.C.).

Present Address

[§]Dmitri Y. Petrovykh: International Iberian Nanotechnology Laboratory (INL), Avenida Mestre José Veiga, 4715-330 Braga, Portugal.

Notes

The authors declare no competing financial interest.

ACKNOWLEDGMENTS

This work was supported by the Office of Naval Research (ONR) and the Air Force Office of Scientific Research (AFOSR). The authors thank Michael Malito (NOVA Research) for his assistance in the design and fabrication of the PTFE chamber. Kenan P. Fears thanks the National Research Council for a Postdoctoral Fellowship at the Naval Research Laboratory (NRL) during the initial stages of this project.

REFERENCES

(1) Weidner, T.; Apte, J. S.; Gamble, L. J.; Castner, D. G. *Langmuir* **2010**, *26*, 3433.
(2) Weidner, T.; Breen, N. F.; Li, K.; Drobny, G. P.; Castner, D. G. *Proc. Natl. Acad. Sci. U.S.A.* **2010**, *107*, 13288.
(3) Mirau, P. A.; Naik, R. R.; Gehring, P. *J. Am. Chem. Soc.* **2011**, *133*, 18243.
(4) Shemetov, A. A.; Nabiev, I.; Sukhanova, A. *ACS Nano* **2012**, *6*, 4585.
(5) Sastry, M.; Brown, C.; Wagner, G.; Clark, T. D. *J. Am. Chem. Soc.* **2006**, *128*, 10650.
(6) Kulp, J. L., III; Clark, T. D. *Chem.—Eur. J.* **2009**, *15*, 11867.
(7) Clark, T. D.; Sastry, M.; Brown, C.; Wagner, G. *Tetrahedron* **2006**, *62*, 9533.
(8) Kulp, J. L., III; Owrutsky, J. C.; Petrovykh, D. Y.; Fears, K. P.; Lombardi, R.; Nafie, L. A.; Clark, T. D. *Biointerphases* **2011**, *6*, 1.
(9) Meier, K.; van, G. W. F. *J. Phys. Chem. A* **2010**, *114*, 1852.
(10) Greenfield, N. J.; Fasman, G. D. *Biochemistry* **1969**, *8*, 4108.
(11) Sreerama, N.; Woody, R. W. *Anal. Biochem.* **2000**, *287*, 252.
(12) Capriotti, L. A.; Beebe, T. P.; Schneider, J. P. *J. Am. Chem. Soc.* **2007**, *129*, 5281.
(13) Stevens, M. M.; Flynn, N. T.; Wang, C.; Tirrell, D. A.; Langer, R. *Adv. Mater. (Weinheim, Ger.)* **2004**, *16*, 915.
(14) Li, T.; Park, H. G.; Lee, H.-S.; Choi, S.-H. *Nanotechnology* **2004**, *15*, S660.
(15) Read, M. J.; Burkett, S. L. *J. Colloid Interface Sci.* **2003**, *261*, 255.
(16) Nygren, P.; Lundqvist, M.; Broo, K.; Jonsson, B.-H. *Nano Lett.* **2008**, *8*, 1844.
(17) Slocik, J. M.; Naik, R. R. *Chem. Soc. Rev.* **2010**, *39*, 3454.
(18) Laera, S.; Ceccone, G.; Rossi, F.; Gilliland, D.; Hussain, R.; Siligardi, G.; Calzolai, L. *Nano Lett.* **2011**, *11*, 4480.
(19) Vermeer, A. W. P.; Norde, W. *J. Colloid Interface Sci.* **2000**, *225*, 394.
(20) Gallardo, I. F.; Webb, L. J. *Langmuir* **2012**, *28*, 3510.
(21) McMillin, C. R.; Walton, A. G. *J. Colloid Interface Sci.* **1974**, *48*, 345.
(22) Blondelle, S. E.; Ostresh, J. M.; Houghten, R. A.; Perez-Paya, E. *Biophys. J.* **1995**, *68*, 351.
(23) Shimizu, M.; Kazutoshi, K.; Morii, H.; Mitsui, K.; Knoll, W.; Nagamune, T. *Biochem. Biophys. Res. Commun.* **2003**, *310*, 606.
(24) Hylton, D. M.; Shalaby, S. W.; Latour, R. A. *J. Biomed. Mater. Res., Part A* **2005**, *73A*, 349.
(25) Fears, K. P.; Latour, R. A. *Langmuir* **2009**, *25*, 13926.
(26) Sivaraman, B.; Fears, K. P.; Latour, R. A. *Langmuir* **2009**, *25*, 3050.
(27) Fears, K. P.; Sivaraman, B.; Powell, G. L.; Wu, Y.; Latour, R. A. *Langmuir* **2009**, *25*, 9319.
(28) Petrovykh, D. Y.; Kimura-Suda, H.; Tarlov, M. J.; Whitman, L. J. *Langmuir* **2004**, *20*, 429.
(29) Jewett, S.; Zemlyanov, D.; Ivanisevic, A. *Langmuir* **2011**, *27*, 3774.
(30) Petrovykh, D. Y.; Kimura-Suda, H.; Whitman, L. J.; Tarlov, M. J. *J. Am. Chem. Soc.* **2003**, *125*, 5219.
(31) Damodaran, S. *Anal. Bioanal. Chem.* **2003**, *376*, 182.
(32) Seah, M. P.; Gilmore, L. S.; Beamson, G. *Surf. Interface Anal.* **1998**, *26*, 642.
(33) Lorenzi, G. P.; Paganetti, T. *J. Am. Chem. Soc.* **1977**, *99*, 1282.
(34) Lorenzi, G. P.; Tomasic, L. *J. Am. Chem. Soc.* **1977**, *99*, 8322.
(35) Hoang, H. N.; Abbenante, G.; Hill, T. A.; Ruiz-Gómez, G.; Fairlie, D. P. *Tetrahedron* **2012**, *68*, 4513.
(36) Wu, Y.; Huang, H. W.; Olah, G. A. *Biophys. J.* **1990**, *57*, 797.
(37) Burck, J.; Roth, S.; Wadhwani, P.; Afonin, S.; Kanithasen, N.; Strandberg, E.; Ulrich, A. S. *Biophys. J.* **2008**, *95*, 3872.
(38) Dill, K. A.; Bromberg, S. *Molecular Driving Forces: Statistical Thermodynamics in Chemistry and Biology*; Garland Science: New York, 2002.
(39) Lide, D. *CRC Handbook of Chemistry and Physics*, 88th ed.; CRC Press: Boca Raton, FL, 2007.
(40) Apte, J. S.; Collier, G.; Latour, R. A.; Gamble, L. J.; Castner, D. G. *Langmuir* **2010**, *26*, 3423.
(41) Feyer, V.; Plekan, O.; Ptasinska, S.; Iakhnenko, M.; Tsud, N.; Prince, K. C. *J. Phys. Chem. C* **2012**, *116*, 22960.
(42) Metwalli, E.; Haines, D.; Becker, O.; Conzone, S.; Pantano, C. G. *J. Colloid Interface Sci.* **2006**, *298*, 825.
(43) Kurth, D. G.; Bein, T. *Langmuir* **1993**, *9*, 2965.
(44) Fears, K. P.; Petrovykh, D. Y.; Clark, T. D. *Biointerphases* 2013, in press.